

Table 1. Background of patients with multiple tumors

Median follow-up (mo)	58 (38–105)
Median age (y)	48 (27–81)
Tumor number (n)	
2	30
3	4
Tumor location (n)	
Same quadrant	22
Next quadrant	10
Opposite quadrant	2
Diagnosis of multiple lesions (n)	
Preoperative	26
Intraoperative	8

tumors was not larger than those of the 35 patients with MMIBC treated by mastectomy (21.2 ± 7.0 mm in the BCT group vs. 24.8 ± 9.1 mm in the mastectomy group, $p = 0.07$). Microcalcification was observed in 12 (34%) of the 35 patients in the mastectomy group.

In the patients with MMIBC treated by BCT, tumor multiplicity was detected before surgery in 26 patients and during surgery in 8 patients. The patient characteristics, such as age, number of tumors, and tumor distribution, are shown in Table 1. The distance between each tumor was recorded in only 5 cases and therefore could not be pre-

sented as a reliable average or median value. Mammography and ultrasonography are presented for representative cases of multicentric/multifocal disease (Fig. 1).

Breast-conserving therapy at our institute basically consists of wide excision of the primary tumor followed by postoperative breast RT. All patients underwent wide excision and axillary dissection. Surgical clips were placed at the surgical margins during surgery for later use as a landmark to determine the boost irradiation field. RT was initiated within 8 weeks after surgery. A total of 50 Gy was delivered to the whole breast in 2-Gy fractions during a 5-week period by opposing tangential fields. Conserved breasts were treated with either ^{60}Co γ -rays or 6-MV X-rays, which was adequate for the breast size. CT simulation was used for treatment planning. For patients with close or positive resection margins, defined as cancer cells observed within 5 mm of the resection margin, boost RT was delivered. The dose of boost RT was fixed to 10 Gy regardless of the shortest distance from the resection margin. The boost RT covered the breast tissue within 3 cm from the clips with positive or close margins. Electron beam RT was usually used. The depth of the anterior chest wall was measured on CT simulation, and the energy was chosen so that the anterior chest wall received 80% of the prescribed dose. If the required energy exceeded 13 MeV, tangential photon

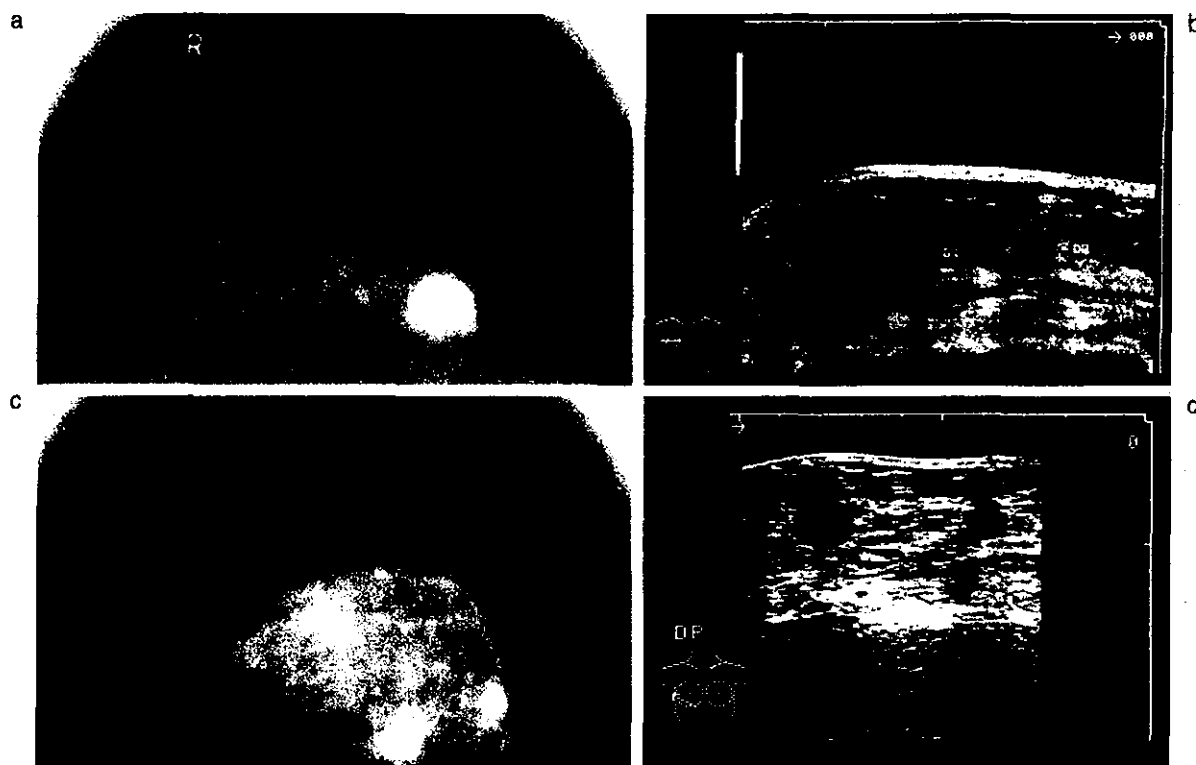


Fig. 1. (a) Mammogram and (b) ultrasound scan of 71-year-old patient who presented with two tumors in right upper-outer quadrant. Diameter of larger and smaller tumors and distance between the two was 20.8 mm, 7.5 mm, and 11.7 mm, respectively. Continuity was found on histologic examination. (c) Mammogram and (d) ultrasound scan of 50-year-old patient who presented with two tumors in right upper-inner quadrant. Diameter of larger and smaller tumors and distance between the two was 21 mm, 10 mm, and 37 mm, respectively. No continuity was found on histologic examination.

beams were used. The same policy and method were applied to both MMIBC and single lesions. The RT method was presented in detail in our previous publication (14, 15). Of 21 MMIBC patients with close or positive margins, 19 received electron boost with energy of 7–13 MeV. One patient with extensive margin involvement received 62 Gy to the whole breast RT using ^{60}Co γ -rays. The remaining 1 patient with close margins (5 mm) did not receive boost RT.

All patients underwent systemic chemotherapy in the form of tamoxifen and 5-fluorouracil for 2 years after surgery. This was initiated after surgery and before RT. No additional systemic therapy was given until breast cancer recurrence was confirmed.

Local control and disease-free survival was estimated by the Kaplan-Meier method. Statistical analysis was performed using the Stat-View program. The cosmetic result was evaluated using the global cosmetic score (8, 16). Patients were divided into two groups according to the cosmetic result: excellent to good and fair to poor. Cosmesis was also analyzed by the chi-square test. $p < 0.05$ was defined as statistically significant.

RESULTS

After wide excision, 21 (62%) of the 34 patients with MMIBC and 167 (28%) of the 594 patients with single lesions had a close surgical margin. The difference was statistically significant ($p < 0.001$). However, the boost irradiation field size was not significantly different between the two groups ($71 \pm 54.6 \text{ cm}^2$ for multiple disease and $64 \pm 30.7 \text{ cm}^2$ for single disease, $p = 0.42$). Patient age, estrogen receptor status, pathologic T and N stage, and tumor pathologic findings were not significantly different between the two groups (Table 2). Of the 34 MMIBC patients and 564 single-lesion patients, 6 (18%) and 126 (21%), respectively, had extensive intraductal component-positive tumors. The difference was not statistically significant.

Pathologic examination demonstrated microscopic continuity between individual tumors in 20 patients (multifocal) and no continuity in 12 patients (multicentric). The information was insufficient for the remaining 2 patients (Table 3).

The median follow-up period for the patients with MMIBC was 58 months (range, 38–105 months). One patient (2.9%) with MMIBC had local recurrence 98 months after BCT. The patient was 41 years old at diagnosis, and the tumors were pathologically Stage IIB (pT2N1M0), extensive intraductal component negative, and margin positive. The recurrence occurred as a solitary nodule near one of the primary lesions. The patient was salvaged by simple mastectomy and was disease free at the latest follow-up visit. Two of the patients with MMIBC (6.5%) developed distant metastases. One patient had bone metastasis 27 months after BCT, the other patient had lung metastasis 39 months after BCT. Of the 564 patients with single lesions, 15 (2.4%) had local recurrence. Consequently, the 5-year

Table 2. Patient characteristics

Characteristic	MMIBC	Single lesions	<i>p</i>
Median age (y)	48 ± 12	50 ± 10	0.26
Pathologic T stage (n)			
pT1	14 (41)	322 (54)	0.30
pT2	20 (59)	270 (45)	
Pathologic N stage (n) (UICC)			
N0	21 (62)	434 (73)	0.14
N1	13 (38)	144 (24)	
N2	0	16 (2)	
Histologic type (n)			
Invasive ductal carcinoma	29 (85)	511 (86)	0.60
DCIS	0	22 (4)	
Invasive lobular carcinoma	3 (9)	27 (5)	
Other	2 (6)	34 (6)	
ER positive (n)	22/34 (65)	306/594 (52)	0.52
EIC positive (n)	5/34 (15)	126/594 (21)	0.86
Close/positive margin (mm)	21/34 (62)	160/594 (27)	<0.01
≥2 to ≤5	8/34 (24)	50/594 (8)	<0.01
>0 to ≤2	7/34 (21)	53/594 (9)	0.02
0	6/34 (18)	57/594 (10)	0.13
Mean boost field size (cm ²)	71 ± 55	65 ± 31	0.46

Abbreviations: UICC = International Union Against Cancer; DCIS = ductal carcinoma in situ; ER = estrogen receptor; EIC = extensive intraductal component; MMIBC = Macroscopically multiple ipsilateral breast cancer; Numbers in parentheses are percentages.

local control rate was 100% for patients with MMIBC and 97% for patients with a single lesion. The difference in local control was not statistically significant between the two groups (Fig. 2). The 5-year disease-free survival rate was 93% for patients with MMIBC and 90% for patients with a single lesion, also not a statistically significant difference (Fig. 3).

Regarding the cosmetic results, we compared the ratio of patients with an excellent to good cosmetic score at 2 years of follow-up between the two groups. Twenty-six (79%) of 33 patients with MMIBC and 444 (81%) of 545 with single lesions had an excellent to good score. Again, the difference was not statistically significant ($p = 0.70$).

DISCUSSION

Macroscopically multiple ipsilateral breast cancer includes both multicentric disease and multifocal disease.

Table 3. Location of multiple tumors and continuity on histologic examination

Location	Continuity		
	Yes	No	Unknown
Same quadrant (n = 22)	14	8	0
Next quadrant (n = 10)	6	3	1
Opposite quadrant (n = 2)	0	1	1

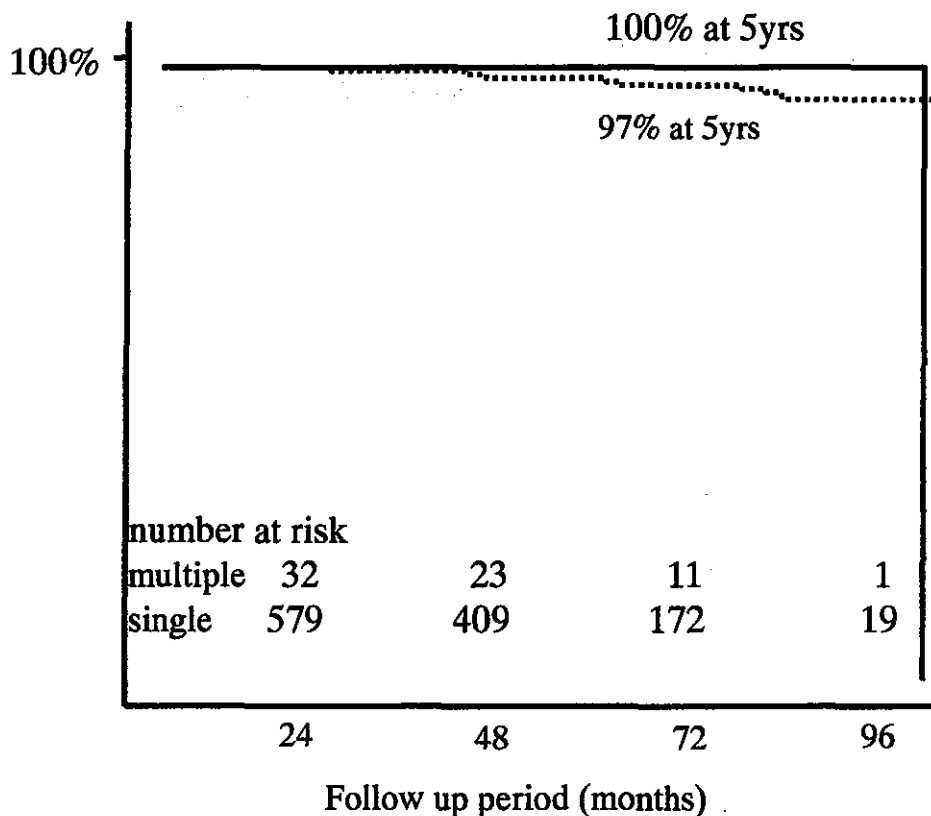


Fig. 2. Local control for macroscopically multiple ipsilateral breast cancer (solid line) and single disease (dashed line). No statistically significant differences were found ($p = 0.8$).

Multifocality and multicentricity were originally pathologic terms and should be discussed from a pathologic point of view. In the currently accepted terminology, multifocality represents the presence of multiple foci of the same tumor, and multicentricity suggests different primary tumors in the same breast (17). Although some researchers have tried to identify such continuity preoperatively using helical CT and/or MRI, these diagnostic imaging modalities are not sufficiently reliable. From a practical point of view, it is generally considered that multifocal tumors are those within the same quadrant and multicentric tumors are those in different quadrants. However, our results indicate that this approximation is not always accurate, because 8 (36%) of 22 tumors that were located in the same quadrant had no apparent continuity on histologic examination.

According to the guidelines for BCT, such as the National Institutes of Health consensus statement, MMIBC is excluded from the indications for BCT (7). A high incidence of local recurrence in early series and a deterioration in the cosmetic result caused by removal of a large amount of the breast tissue were the main reasons for this recommendation. A study by Fowble *et al.* (18), in which the pathologic review of the mastectomy specimens revealed extensive residual disease in three or four quadrants of the breast after excisional biopsy in 50% of the patients with MMIBC, supports this recommendation further.

Some previous reports regarding BCT for MMIBC have

been published (Table 4). Kurtz *et al.* (9), Leopold *et al.* (10), and Wilson *et al.* (11) reported a high local recurrence rate for patients with MMIBC who underwent BCT (23–40%). In their studies, the surgical margin status was insufficient or not fully examined (9–11). Kurtz *et al.* (9) reported that the local recurrence rate in 22 patients with clearly adequate margins was low (1 of 22 or 4.5%) and in 39 patients with unknown or positive margins it was very high (14 of 39 or 36%). Hartsell *et al.* (12) reported a good local control rate (local recurrence rate 3.7%), and in their study, the close (<1 mm) or positive margin rate was only 22% (6 of 27). In a recent study by Cho *et al.* (13), BCT was offered to 15 patients in whom microscopically negative margins were obtained, and none of them had local recurrence at a median follow-up of 77 months. A positive surgical margin is one of the major risk factors for local recurrence (19–21). However, a large surgical margin will reduce the residual breast volume and deteriorate cosmesis, one of the most important goals of BCT (22).

The effectiveness of boost RT to decrease local recurrence has been established in a randomized trial (23). To increase the accuracy of postoperative RT, including boost RT, we placed different-size radiopaque clips at the surgical margin together with radial sectioning of the pathologic specimen. This facilitated identification of a close or positive margin on CT simulation and was useful for determining an adequate boost field (14).

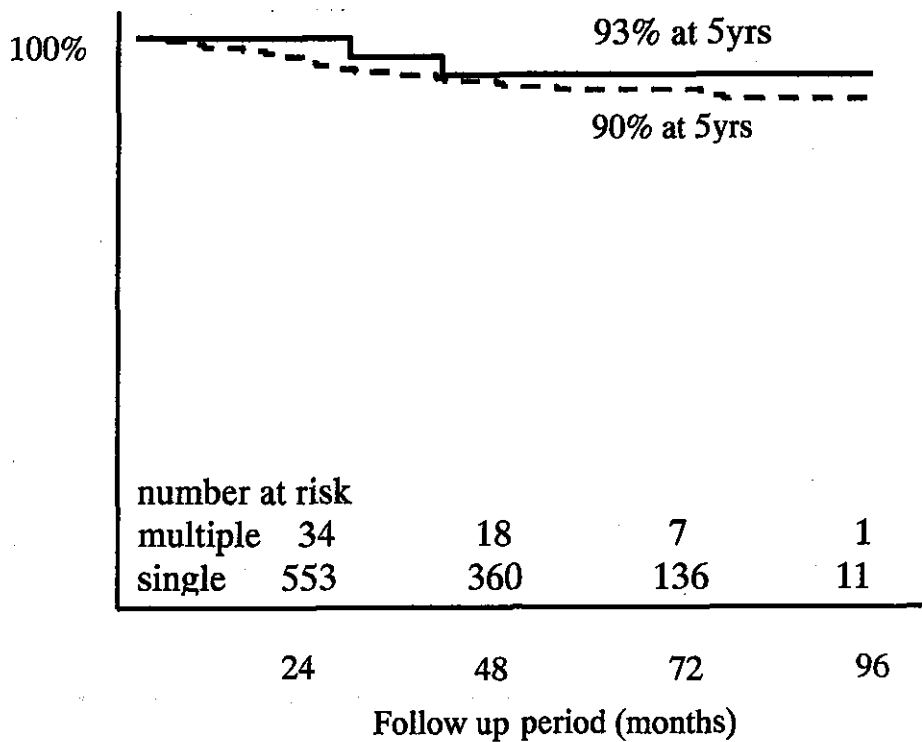


Fig. 3. Disease-free survival between macroscopically multiple ipsilateral breast cancer (solid line) and single disease (dashed line). No statistically significant differences were found ($p = 0.63$).

In our study, 62% of the patients with MMIBC had close surgical margins, significantly greater than that in the patients with single disease, but the local control rate was not significantly different. We believe that meticulous treatment planning using surgical clips and CT simulation ameliorated the local control rate. Moreover, this also facilitated control of the size of the boost field for multiple lesions by avoiding inclusion of “safe” parts of the resection margin. Thus, we believe our boost irradiation technique contributed to the favorable cosmetic result; a large boost dose and volume may deteriorate the cosmetic result (24). The excellent to good cosmetic score rate did not differ significantly between those with multiple and single lesions.

When interpreting these observations, possible ethnic differences between Japan and Western countries, in both the natural history and the patterns of care of breast cancer, should be taken into account. As several researchers have pointed out, Japanese women with breast cancer seem to have a substantially more favorable prognosis than patients in Western countries (25, 26). In our series, the 5-year disease-free survival rate for patients without pathologically positive axillary lymph nodes, with one to three positive nodes, four to nine nodes, and more than nine positive nodes was 95.2%, 94.5%, 76.5%, and 38.9%, respectively (27). In such situations, intensive chemotherapy with significant toxicity is difficult to jus-

Table 4. Results of other trials

	Leopold (1989)	Kurtz (1990)	Wilson (1993)	Hartsell (1994)	Cho (2002)	Our study
Local recurrence (%)	4/10 (40)	15/61 (25)	3/13 (23)	1/27 (3.7)	0/15	1/34 (2.9)
Median follow-up (mo)	64	71	71	53	77	98
Radiotherapy (6y)	45–52 ± boost	50 + boost	50 + boost	45–54 ± boost	45–50 + boost	50 ± boost
Close/positive margin	Not fully examined	Positive 12/61 Unknown 34/61	Not fully examined	6/27 (22)	0/15	21/34 (62)
Chemotherapy	Not done	For some cases	CMF for 6 patients	AC or CMF TAM	AC, CMF or other	TAM, 5-FU

Abbreviations: CMF = cyclophosphamide, methotrexate, and 5-fluorouracil; AC = doxorubicin and cyclophosphamide; TAM = tamoxifen; 5-Fu = 5-fluorouracil.

tify, especially in patients with a small number of lymph node metastases. Consequently, all the patients in the current study received oral 5-fluorouracil, which is reportedly less toxic than cyclophosphamide, methotrexate, and 5-fluorouracil or doxorubicin and 5-fluorouracil as systemic adjuvant therapy. The local control rate for BCT in Japanese women is also excellent, but the difference is less striking than the survival rate. In our series, the 5-year local control rate for patients with negative, close (≤ 5 mm), and positive margins was 98.9%, 96.6%, and

92.2%, respectively (27). Local recurrence was usually detected >3 years after BCT in previous studies of MMIBC, and it occurred 10 years after BCT in our study. Therefore, we need longer follow-up and more observation of different ethnicities to reach a firm conclusion. However, our result at this stage suggests that patients with MMIBC can be candidates for BCT, as long as each tumor is operable by breast-conserving surgery criteria and the close surgical margin is accurately detected and treated with adequate boost RT.

REFERENCES

- Sarrazin D, Le MG, Arriagada R, *et al.* Ten-year results of a randomized trial comparing a conservative treatment to mastectomy in early breast cancer. *Radiother Oncol* 1989;14:177-184.
- van Dongen JA, Bartelink H, Fentiman IS, *et al.* Randomized clinical trial to assess the value of breast-conserving therapy in stage I and II breast cancer, EORTC 10801 trial. *J Natl Cancer Inst Monogr* 1992;11:15-18.
- Blichert-Toft M, Rose C, Andersen JA, *et al.*, for the Danish Breast Cancer Cooperative Group. Danish randomized trial comparing breast conservation therapy with mastectomy: Six years of life-table analysis. *J Natl Cancer Inst Monogr* 1992;11:19-25.
- Fisher B, Anderson S, Redmond CK, *et al.* Reanalysis and results after 12 years of follow-up in a randomized clinical trial comparing total mastectomy with lumpectomy with or without irradiation in the treatment of breast cancer. *N Engl J Med* 1995;333:1456-1461.
- Danoff BF, Haller DG, Glick JH, *et al.* Conservative surgery and irradiation in the treatment of early breast cancer. *Ann Intern Med* 1985;102:634-642.
- Margolese R. Surgical considerations in selecting local therapy. *J Natl Cancer Inst Monogr* 1992;41-48.
- Veronesi U. NIH consensus meeting on early breast cancer. *Eur J Cancer* 1990;26:843-844.
- Winchester DP, Cox JD, for the American College of Radiology, American College of Surgeons, College of American Pathologists, Society of Surgical Oncology. Standards for diagnosis and management of invasive breast carcinoma. *CA Cancer J Clin* 1998;48:83-107.
- Kurtz JM, Jacquemier J, Amalric R, *et al.* Breast-conserving therapy for macroscopically multiple cancers. *Ann Surg* 1990;212:38-44.
- Leopold KA, Recht A, Schnitt SJ, *et al.* Results of conservative surgery and radiation therapy for multiple synchronous cancers of one breast. *Int J Radiat Oncol Biol Phys* 1989;16:11-16.
- Wilson LD, Beinfeld M, McKhann CF, *et al.* Conservative surgery and radiation in the treatment of synchronous ipsilateral breast cancers. *Cancer* 1993;72:137-142.
- Hartsell WF, Recine DC, Griem KL, *et al.* Should multicentric disease be an absolute contraindication to the use of breast-conserving therapy? *Int J Radiat Oncol Biol Phys* 1994;30:49-53.
- Cho LC, Senzer N, Peters GN. Conservative surgery and radiation therapy for macroscopically multiple ipsilateral invasive breast cancers. *Am J Surg* 2002;183:650-654.
- Kokubo M, Mitsumori M, Yamamoto C, *et al.* Impact of boost irradiation with surgically placed radiopaque clips on local control in breast-conserving therapy. *Breast Cancer* 2001;8:222-228.
- Hiraoka M, Mitsumori M, Okajima K, *et al.* Use of a CT simulator in radiotherapy treatment planning for breast conserving therapy. *Radiother Oncol* 1994;33:48-55.
- Harris JR, Levene MD, Svensson G, Hellman S. Analysis of cosmetic results following primary radiation therapy for stages I and II carcinoma of the breast. *Int J Radiat Oncol Biol Phys* 1979;5:257-261.
- Andea AA, Wallis T, Newman LA, *et al.* Pathologic analysis of tumor size and lymph node status in multifocal/multicentric breast carcinoma. *Cancer* 2002;94:1383-1390.
- Fowble B, Yeh IT, Schultz DJ, *et al.* The role of mastectomy in patients with stage I-II breast cancer presenting with gross multifocal or multicentric disease or diffuse microcalcifications. *Int J Radiat Oncol Biol Phys* 1993;27:567-573.
- DiBiase SJ, Komarnicky LT, Schwartz GF, *et al.* The number of positive margins influences the outcome of women treated with breast preservation for early stage breast carcinoma. *Cancer* 1998;82:2212-2220.
- Mansfield CM, Komarnicky LT, Schwartz GF, *et al.* Ten-year results in 1070 patients with stages I and II breast cancer treated by conservative surgery and radiation therapy. *Cancer* 1995;75:2328-2336.
- Wazer DE, Jabro G, Ruthazer R, *et al.* Extent of margin positivity as a predictor for local recurrence after breast conserving irradiation. *Radiat Oncol Invest* 1999;7:111-117.
- Wazer DE, DiPetrillo T, Schmidt-Ullrich R, *et al.* Factors influencing cosmetic outcome and complication risk after conservative surgery and radiotherapy for early-stage breast carcinoma. *J Clin Oncol* 1992;10:356-363.
- Bartelink H, Horiot JC, Poortmans P, *et al.* Recurrence rate after treatment of breast cancer with standard radiotherapy with or without additional radiation. *N Engl J Med* 2001;345:1378-1387.
- Borger JH, Kemperman H, Smitt HS, *et al.* Dose and volume effects on fibrosis after breast conservation therapy. *Int J Radiat Oncol Biol Phys* 1994;30:1073-1081.
- Nemoto T, Tominaga T, Chamberlain A, *et al.* Differences in breast cancer between Japan and the United States. *J Natl Cancer Inst* 1977;58:193-197.
- Yonemoto RH. Breast cancer in Japan and United States: Epidemiology, hormone receptors, pathology, and survival. *Arch Surg* 1980;115:1056-1062.
- Kokubo M, Mitsumori M, Ishikura S, *et al.* Results of breast-conserving therapy for early stage breast cancer: Kyoto University experiences. *Am J Clin Oncol* 2000;23:499-505.

Original Article

Efficacy of 3D-MR Mammography for Breast Conserving Surgery after Neoadjuvant Chemotherapy

Seigo Nakamura*¹, Hironori Kenjo*¹, Takeki Nishio*¹, Toshiki Kazama*², Osamu Doi*² and Koyu Suzuki*³

Background: One of the main roles of neoadjuvant chemotherapy for breast cancer is to shrink large tumors to increase patient eligibility for breast conserving surgery. Three dimensional MR Mammography (3D-MRM) can detect tumor extension more accurately compared with mammography and Ultrasonography (US). Therefore, the shrinkage pattern observed on 3D-MRM was analyzed with regard to several pathological factors.

Methods: A total of 27 breast cancer cases were examined by 3D-MRM before and after neoadjuvant chemotherapy. The volume reduction and shrinkage patterns were assessed and compared with the pathological diagnosis.

Results: There were two shrinkage patterns. Twelve of 25 evaluable breast cancers (48%) showed a concentric shrinkage pattern while 13 cases (52%) showed a dendritic shrinkage pattern. The cases with concentric shrinkage were good candidates for breast conserving surgery, But tumors showing dendritic shrinkage often had positive margins necessitating mastectomy. Pathologically, tumors with a papillotubular pattern, Estrogen receptor (ER) positivity, low nuclear grade and c-erbB 2 negativity tended to show dendritic shrinkage.

Conclusions: 3D-MRM is a useful modality for evaluating whether breast conserving surgery can be safely done in the neoadjuvant setting.

Breast Cancer 9:15-19, 2002.

Key words: 3D-MR Mammography, Neoadjuvant chemotherapy, Breast conserving surgery, MRI

Recently, the response rate of neoadjuvant chemotherapy has become 80-90%, But several large Randomized Clinical Trials (RCT's) have shown no survival benefit even if the regimen was given in the neoadjuvant setting instead of as adjuvant chemotherapy³⁾. On the other hand, the downstaging of the primary tumor allows breast conserving surgery instead of mastectomy, which increases the quality of life for the patient⁴⁾. Therefore, the main role of neoadjuvant chemotherapy is to observe *in vivo* chemosensitivity and to increase the possibility of breast conserving surgery^{5,6)}. During breast conserving surgery, it is important to avoid positive margins, which is a risk factor for local rec-

currence and has the potential to decrease survival^{7,8)}. Three-dimensional MR Mammography (3D-MRM) allows observation of the cancerous lesion from any direction and estimation of the lesion's volume^{8,9)}. 3D-MRM can detect tumor extension more accurately than mammography or US^{10,12)}. In the neoadjuvant setting, it is more difficult to identify extension of the residual tumor¹³⁾. Therefore, 3D-MRM before and after neoadjuvant chemotherapy was performed and the tumor shrinkage pattern was analyzed with respect to pathological characteristics.

Materials and Methods

A total of 27 breast cancer cases were examined by 3D-MRM before and after neoadjuvant chemotherapy. The volume reduction and shrinkage patterns were analyzed and compared with the pathological diagnosis. The 3D-MRM protocol at St. Luke's International hospital is shown in Table 1. The neoadjuvant chemotherapy regimen was CEF

*¹Department of Surgery, *²Department of Radiology, and *³Department of Clinical Pathology, St. Luke's International Hospital, Japan.
Reprint requests to Seigo Nakamura, Department of Surgery, St. Luke's International Hospital, 9-1 Akashi-cho, Chuoku, Tokyo 104-0044, Japan.

Abbreviations:

US, Ultrasonography; ER, Estrogen receptor; RCT, Randomized Clinical Trial; CR, Complete response

Received July 19, 2001; accepted December 3, 2001

Table 1. Sequence of 3D-MRM at St. Luke's International Hospital

MRI: GE SIGNA 1.5T
Coil: Breast phased array coil
Settings: EFGRE 3D (Enhanced Fast Gradient Echo 3D)
TR 6.7 ms, TE 1.7 ms, TI 40 ms,
FA15° 256 × 160 matrix,
Slice thickness 1 mm, FOV: 16 cm
Gd enhancement by auto-infuser pump
(Gd 0.2 mmol/kg, Infusion speed 1 ml/sec)
Scan option: SPECIAL (Special Inversion at lipids)
(Scan begins 45 seconds after Gd injection)
Whole transaction time: about 90 seconds

(cyclophosphamide 100 mg orally for 14 days, epirubicin 40 mg/m² and 5-FU 500 mg/m² intravenously every 3 weeks) for 4 cycles to 5 cases, Docetaxel (60 mg/m² intravenously every 3 weeks) for 4 cycles for 10 cases and AT (THP-adriamycin 50 mg/m² and Docetaxel 60 mg/m² intravenously) for 4 cycles for 12 cases. The pathological diagnosis including ER, PgR, nuclear grade and C-erbB 2 status was obtained by core biopsy before neoadjuvant chemotherapy. 3D-MRM was performed before and after neoadjuvant chemotherapy for each case. The shrinkage pattern after neoadjuvant chemotherapy was assessed and compared with the pathological results.

Results

The shrinkage patterns were divided into two types. One type was concentric which means the tumor shrank from all directions toward the center. The other type was dendritic which means the tumor still retained a dendritic shape in the original area even if the tumor was markedly reduced in volume. The overall response rate (CR + PR, %) was 88.9%. One case was progressive disease and was removed from evaluation. Another case showed Complete Respnce (CR) by 3D-MRM which was also removed from evaluation. Among the evaluated 25 cases, 12 cases (48%) showed concentric and 13 cases (52%) showed dendritic type shrinkage (Fig 1). Typical concentric type shrinkage is shown in Fig 2. Fig 3 shows a dendritic type shrinkage pattern, for which mastectomy was performed because of positive margin after breast conserving surgery. Fig 4A appeared to have concentric shrinkage by US and 2-D MRM, but showed dendritic shrinkage on 3D-MRM (Fig 4B). Fig 5 was another lesio with dendritic type shrinkage. The dumbbell-shaped

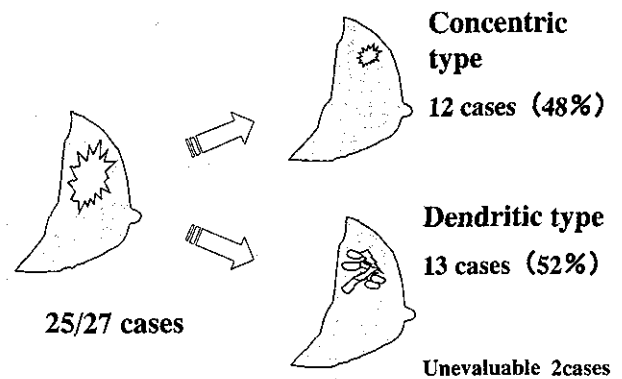


Fig 1. All neoadjuvant cases were divided into 2 groups according to shrinkage pattern.

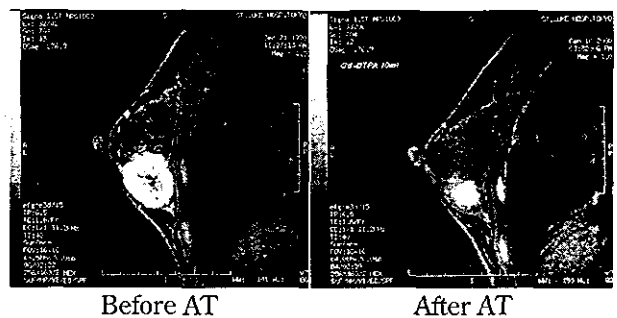


Fig 2. Concentric shrinkage; BCT with negative margin and good cosmesis.

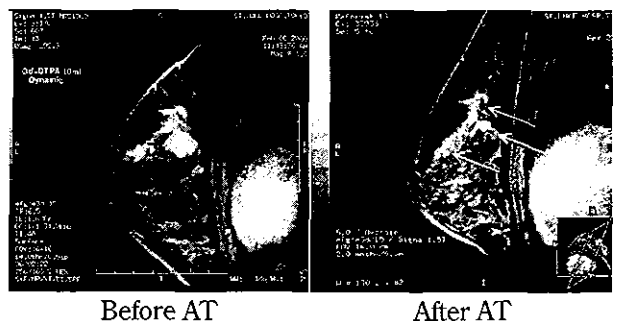


Fig 3. Dendritic shrinkage; BCT → Mastectomy (CR by palpation, however, marked residual lesions).

tumor shrank markedly as if it were a solitary small round tumor, but, it had an extensive intraductal component necessitating careful evaluation for breast conserving surgery. The shrinkage pattern by pathological type is shown in Fig 6.

Papillotubular carcinoma more frequently showed observed in dendritic type shrinkage. Two invasive lobular carcinomas showed dendritic shrinkage. Scirrhous carcinoma most frequently showed concentric type shrinkage. The comparison between shrinkage pattern and nuclear grade

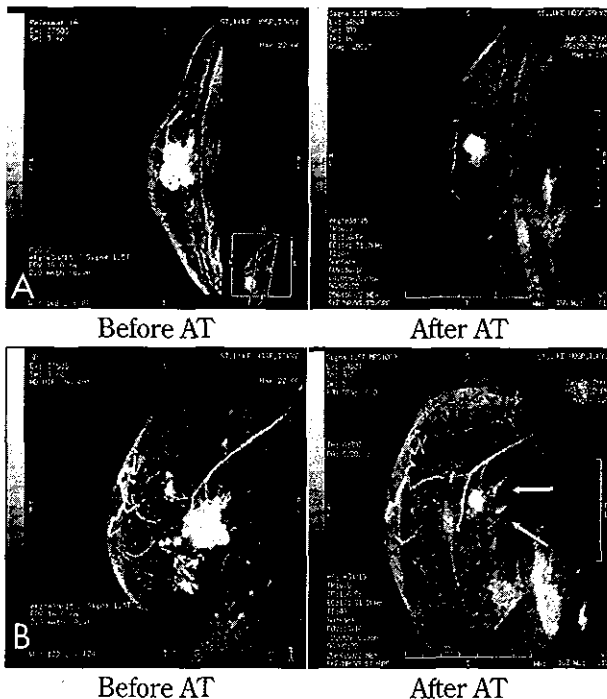


Fig 4. (A) 2D-MRM image showed concentric shrinkage. (B) 3D-MRM of the same case clearly showed intraductal spread, was dendritic shrinkage.

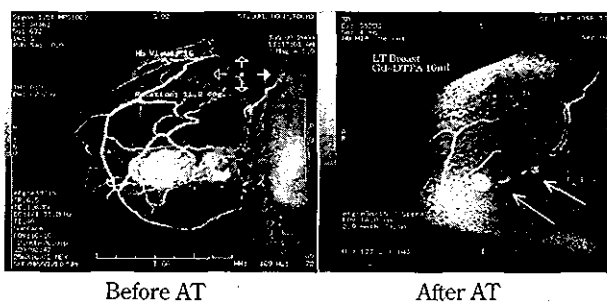


Fig 5. 3D-MRM shows dendritic shrinkage after neoadjuvant chemotherapy.

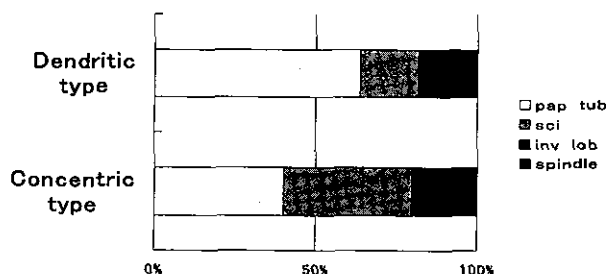


Fig 6. Shrinkage pattern and histological type. Pup.tub., papillotubular type (invasive ductal cancer which tends to retain papillotubular structure); sci., scirrhous type (invasive ductal cancer which tends to spread randomly to the interstitial space); inv.lob., invasive lobular type.

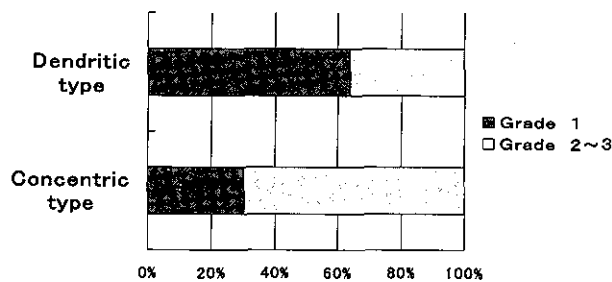


Fig 7. Shrinkage pattern and nuclear grade.

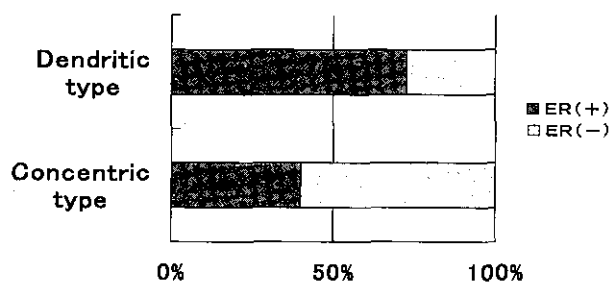


Fig 8. Shrinkage pattern and estrogen receptor.

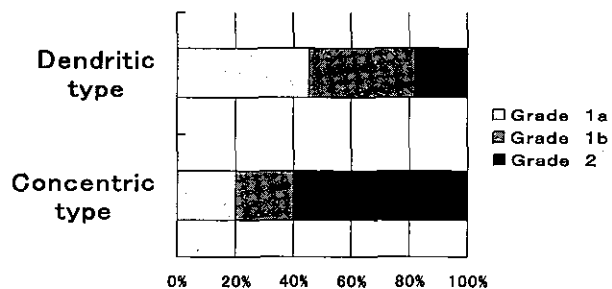


Fig 9. Shrinkage pattern and histological effect by chemotherapy.

is shown in Fig 7. High grade tumors (Grade 2 and 3) tended to show concentric shrinkage. In contrast, low grade tumors more often showed dendritic shrinkage. ER (+) tumors tended to shrink as dendritically (Fig 8). ER (-) tumors tended to more often shrink concentrically. Among tumors showed concentric shrinkage which generally means marked reduction of tumor volume, there were several cases of Grade 1a (mild response) response according to the histopathological criteria for assessment of therapeutic response by the Japanese Breast Cancer Society (Fig 9).

Discussion

3D-MRM is a useful modality for preoperative staging in the management of breast cancer and especially for detecting the tumor extension^{14,18)}. Esserman *et al*, reported that MRM correctly identified residual or primary cancer in 55 of 58 cases and accurately predicted the extent of the cancer in 54 of 58 cases. The anatomic extent was more accurately defined with MRM than with Mammography (98% vs 55%)¹⁰⁾. Our data also suggest that 3D-MRM could detect extensive intraductal component more accurately than mammography and US (82.5% vs. 62.1% vs. 66.7%, respectively)⁹⁾. In the neoadjuvant setting, it was more difficult to assess the pathological effect by mammography¹³⁾. Abraham *et al*, reported 30 of 31 mastectomy cases (97%) after neoadjuvant chemotherapy were correctly assessed residual tumor by 3D-MRM¹⁹⁾. Therefore, 3D-MRM was used to evaluate residual tumor patterns after neoadjuvant chemotherapy^{20, 21)}. Dendritic and concentric type shrinkage patterns occur with about equal frequency after neoadjuvant chemotherapy, which means about half of the cases after neoadjuvant chemotherapy should be cautiously evaluated for breast conserving surgery. The long-term results of the NSABP-18 trial showed the risk of local failure was greatest in those patients who originally were thought to require a mastectomy but whose disease was downstaged sufficiently by neoadjuvant chemotherapy to undergo lumpectomy (10 of 69, 14.5%) 3D-MRM can avoid positive margins and will eventually achieve the same local control rate as ordinal breast conserving surgery. Our data suggest that tumors showing poor prognostic factors including ER negativity and high nuclear grade (2 and 3) tend to shrink concentrically. On the other hand, ER (+), low nuclear grade and papillotubular cancer (invasive ductal cancer which has a partly ductal structure) tend to show dendritic shrinkage, which indicates ductal spread. Care regarding positive margins during breast conserving surgery is necessary in the latter case. 3D-MRM and several biological markers (ER, Ki-67, c-erbB2 etc.) have the potential to predict the shrinkage pattern and the indication for neoadjuvant chemotherapy. However, the number of the evaluated cases in this study was too small, so further data and multivariate analysis is necessary in the future.

Acknowledgement

This study was supported by a grant for scientific research expense for Health and Welfare Program (Chairman; Goi Sakamoto, M.D., Cancer Institute, Tokyo) from the ministry of Health and Welfare in Japan.

References

- 1) Fisher B, Bryant J, Walmark N, *et al*: Effect of preoperative chemotherapy on the outcome of women with operable breast cancer. *J Clin Oncol* 16:2672-2685, 1998.
- 2) Fisher B, Brown A, Mamounas E: Effect of preoperative chemotherapy on local-regional disease in women with operable breast cancer: Findings from National Surgical Adjuvant Breast and Bowel Project B-18. *J Clin Oncol* 15:2483-2493, 1997.
- 3) Makris A, Powles TJ, Ashley SE, *et al*: A reduction in requirements for mastectomy in a randomised trial of neoadjuvant chemoendocrine therapy in primary breast cancer. *Ann Oncol* 9:1179-1184, 1998.
- 4) McMasters KM, Hunt KK: Neoadjuvant chemotherapy, locally advanced breast cancer, and quality of life. *J Clin Oncol* 17:441-444, 1999.
- 5) Trecate G, Ceglia E, Stabile F, *et al*: Locally advanced breast cancer treated with primary chemotherapy: comparison between magnetic resonance imaging and pathological evaluation of residual disease. *Tumori* 85:220-228, 1999.
- 6) Stebb J, Gaya A: The evidence-based use of induction chemotherapy in breast cancer. *Breast Cancer* 18:23-37, 2001.
- 7) Asher M, Jones P, Prosnitz L, *et al*: Local failure and margin status I early-stage breast carcinoma treated with conservation surgery and radiation therapy. *Ann Surg* 218:22-28, 1993.
- 8) Fortin A, Larochelle M, Laverdiere J, *et al*: Local failure is responsible for the decrease in survival for patients with breast cancer treated with conservative surgery and postoperative radiotherapy. *J Clin Oncol* 17:10-109, 1999.
- 9) Nakamura S, Sugiura S, Nishio T, *et al*: Three dimensional MRI for indication of breast conserving surgery. XXX World Congress of the International College of Surgeons (abstr) 1507-1511, 1996.
- 10) Esserman L, Hylton N, Yssa L, *et al*: Utility of magnetic resonance imaging in the management of breast cancer: evidence for improved preoperative staging. *J Clin Oncol* 17:110-119, 1999.
- 11) Schinitt SJ, Connolly JL, Harris JR, *et al*: Pathologic prediction of early local recurrence in stage I and II breast cancer treated by primary radiation therapy. *Cancer* 53:1049-1057, 1984.
- 12) Harms SE, Flamig DP, Evans WP, *et al*: MR imaging of the breast; Current status and future potential. *AJR* 163:1039-1047, 1994.
- 13) Vinnicombe SJ, MacVicar AD, Guy RL, *et al*: Primary Breast Cancer: Mammographic changes after neoadjuvant chemotherapy, with pathological correlation. *Radiology* 198:333-340, 1996.
- 14) Pierce WB, Harms SE, Flamig DP, *et al*: Three-dimensional Gadolinium-enhanced MR imaging of the breast. *Radiology* 181:757-763, 1991.

- 15) Stelling CB. MR imaging of the breast for cancer evaluation. *Radiologic Clinics of North America* 33:1187-1204, 1995.
- 16) Jeffrey CW, Gillian N: MR imaging of the Breast. *Radiology* 196:593-610, 1995.
- 17) Nakamura S: Three dimensional MRI for breast conserving surgery. *Jpn J Cancer Clin* 46:587-591, 2000 (in Japanese with English Abstract).
- 18) Nakamura S, Sugiura K, Nishio T, *et al*: Three-dimensional MRI for indication of breast conserving surgery. *Jpn J Breast Cancer* 11(4):679-685, 1996 (in Japanese with English Abstract).
- 19) Abraham DC, Jones RC, Jones SE, *et al*: Evaluation of neoadjuvant chemotherapeutic response of locally advanced breast cancer by magnetic resonance imaging. *Cancer* 78:91-100, 1996.
- 20) Harms SE: Breast Magnetic Resonance Imaging. *Seminars in CT and MRI* 19:104-120, 1998.
- 21) Harms SE: Integration of breast magnetic resonance imaging with breast cancer treatment. *Topics in Magnetic resonance imaging* 9:79-91, 1998.

Report from the Study Group

3D Imaging of Intraductal Spread of Breast Cancer and Its Clinical Application for Navigation Surgery

Yasuhiro Tamaki^{*1}, Sadako Akashi-Tanaka^{*2}, Takanori Ishida^{*3}, Takayoshi Uematsu^{*4}, Mikihiro Kusama^{*5}, Yuka Sawai^{*6}, Seigo Nakamura^{*7}, Kazufumi Hisamatsu^{*8}, Yoshiro Tanji^{*1}, Yoshinobu Sato^{*9}, and Nariaki Matsuura^{*10}, Study Group for 3D-Imaging Diagnosis of Intraductal Component of Breast Cancer

^{*1}Department of Surgical Oncology, Osaka University Graduate School of Medicine, ^{*2}Division of Breast Surgery, National Cancer Center Hospital, ^{*3}Division of Surgical Oncology, Graduate School of Medicine, Tohoku University, ^{*4}Division of Diagnostic Radiology, Shizuoka Cancer Center Hospital, ^{*5}Third Department of Surgery, Tokyo Medical University, ^{*6}Department of Diagnostic Radiology, Osaka Medical Center for Cancer and Cardiovascular Diseases, ^{*7}Department of Surgery, St. Luke's International Hospital, ^{*8}Department of Surgery, Hiroshima City Asa Hospital, ^{*9}Division of Interdisciplinary Image Analysis, Department of Medical Robotics and Image Sciences, Osaka University Graduate School of Medicine, and ^{*10}Department of Pathology, School of Allied Health Sciences, Faculty of Medicine, Osaka University, Japan.

Background: To perform optimal tumor resection of breast cancer, preoperative information concerning intraductal spread of cancer (ISC) is very important.

Methods: To detect ISC, three-dimensional (3D) imaging methods including helical CT, MRI, and ultrasound were examined in patients with primary breast cancer by comparison with multi-sliced pathological specimens.

Results: The sensitivity of each modality for detecting ISC was 64.7%, 90.2% and 78.6%, and the specificity was 97.1%, 62.9% and 100%, respectively. Subsequently, the potential of each modality for navigation in breast conserving surgery was assessed. Three-dimensional helical CT navigation could reduce the positive rate of the specimen margins, and 3D MRI navigation using a special mapping sheet enabled removal of non-palpable breast cancer without positive margins in 66.7% of patients preliminarily. Real-time 3D ultrasound images correlated with the resected tumor size, with the difference between the two less than 2 cm in 72.7% of the patients with ISC.

Conclusion: Three-dimensional images from each modality were reliable enough for diagnosis of tumor spread, and surgical navigation using these images seemed to have potential clinical application for breast conserving surgery. Prospective studies for navigation surgery with more patients are needed.

Breast Cancer 9:289-295, 2002.

Key words: 3D, MRI, CT, Ultrasound, Intraductal spread, EIC, Breast cancer, Navigation

Breast conserving surgery has been a standard operation for small breast tumors. This surgery was originally developed to improve cosmetic outcome and patients' quality of life after breast cancer surgery. To achieve better cosmesis, a minimal resection of tumor is needed. This, however, must often leads to positive or close surgical margins, and increases local recurrence in the conserved breast¹⁾. Positive surgical margins are generally caused by the existence of intraductal spread of cancer (ISC) and technical failure, for

examples, disorientation of tumor margins by a surgeon²⁾. The diagnosis of ISC by mammography and ultrasonography has been studied for years. However, these diagnostic images are 2-dimensional (2D), and surgeons perform tumor resection according to 3-dimensional (3D) images reconstructed in their minds. If 3D images can be obtained before surgery and provide a visual representation of cancer spread, opposing goals of minimum resection of the tumor and negative surgical margins could be met. Recently, computer tomography (CT) and magnetic resonance imaging (MRI) with contrast enhanced media are used for diagnosing breast cancer, and are expected to display tumor spreading in the breast. Further-

Reprint requests to Yasuhiro Tamaki, Department of Surgical Oncology, Osaka University Graduate School of Medicine, 2-2-E10, Yamadaoka, Suita, Osaka 565-0871, Japan.
E-mail: tamaki@onsurg.med.osaka-u.ac.jp

more, multi-detector CT (MD-CT) and 3D ultrasonography became available very recently, and can produce 3D images easily.

This study group was organized by the Japanese Breast Cancer Society to investigate 3D imaging of ISC. In this paper, we report the usefulness of these 3D images for diagnosing ISC, and discussed the possibility of intraoperative navigation for breast conserving surgery.

Materials and Methods

Three dimensional images were obtained and analyzed using each modality at each institute. Helical CT scanning to analyze the diagnostic capability for ISC for this technique was performed using an X-Vigor (Toshiba, Tokyo, Japan) or a HiSpeed Advantage (GE Medical Systems, Milwaukee, WI). The X-ray beam thickness was 3-5 mm. Ninety-six to 100 ml of non-ionic contrast media (CE) was injected at a rate of 2 to 4 ml/sec. Thirty to fifty seconds after administration of CE, early-phase scanning was started. Late-phase scanning was performed 120-180 seconds after the injection of CE. Three dimensional images were created from the obtained 2-D images, and assessed using software bundled with the machine.

Three-dimensional MRI assessment of ISC was performed using Magnetom Vision 1.5 T (Siemens Medical Systems, Erlangen, Germany) with a breast phased array coil. Gradient echo fat-suppressed 3D-T1 weighted images were obtained after injection of Gadtrinium-DTPA (0.2 ml/kg) with an interval of 120 seconds. Three-dimensional images of the breast were constructed by the maximum intensity projection (MIP) method.

Ultrasound images were obtained using SONOLINE Elegia (Siemens Ultrasound Japan, Tokyo, Japan) to assess ISC. Volume rendering images were obtained using a 7-9 MHz linear probe, and ISC was detected with multi-planner reconstruction (MPR) images, which are obtained by slanted coronal slices in any angle (Fig 1).

Helical CT navigation was performed using a HiSpeed Advantage (GE Medical Systems, Milwaukee, WI) or ProSpeed SA Libra (GE Yokogawa Medical Systems, Tokyo, Japan) machine. Each patient's skin had been previously marked indicating tumor spread by a surgeon based on palpation of the tumor. Each patient was in the supine position, and a radio-opaque ring was put on the marking by a radiologist. Ninety ml of non-ionic CE was

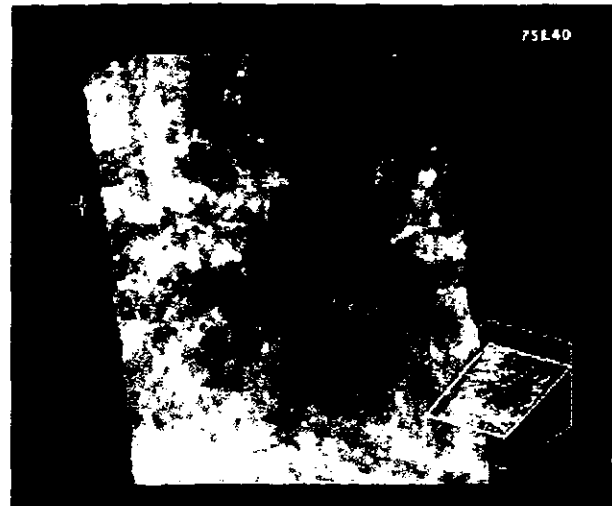


Fig 1. Multi-planner reconstruction image of 3D ultrasound.

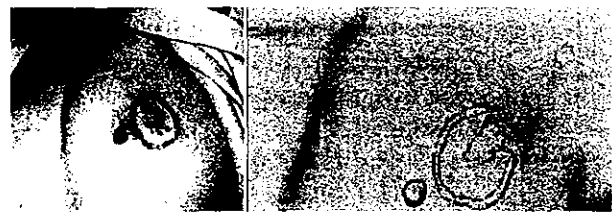


Fig 2. The skin marking for resection made by a surgeon was misaligned, and the marking was adjusted to the correct position according to the 3D helical CT image.

injected intravenously. The X-ray beam thickness was 3 mm, and the scanning was started 70 seconds after giving the CE. The images were analyzed by a commercially available workstation as previously reported³⁾. For this navigation, the shaded surface display method was used. If the marking by a surgeon was misaligned from the area where the tumor spread, the marking was adjusted according to the CT image (Fig 2).

Three dimensional MRI navigation was performed using a SIGNA 1.5T (GE Medical Systems) with a 5-inch surface coil. Patients were in the supine position, and the images were obtained by a fat-suppressed 2D spin echo method using a specially created lattice sheet for mapping of the tumor. The navigation method was detailed in a previous report⁴⁾. Briefly, after obtaining the 3D image of the breast covered by the lattice mapping sheet, the grids containing tumor nests were marked on the breast with a felt pen (Fig 3).

Real-time 3D ultrasound navigation was performed with an SSD 2000 (Aroka, Tokyo, Japan) ultrasound scanner and a 3D locating system. The

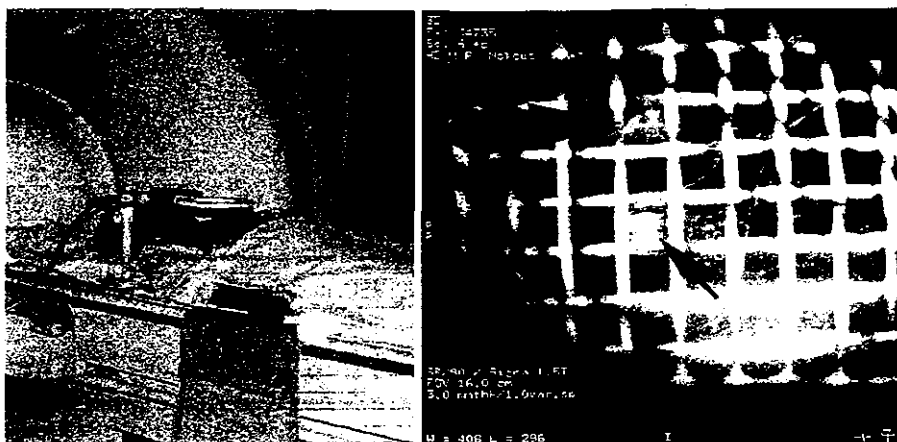


Fig 3. 3D MRI navigation using a specialized mapping sheet. The patient is placed in the supine position (A). The grids containing the tumor (a large arrow) are marked on the skin (B). A small arrow indicates the nipple.

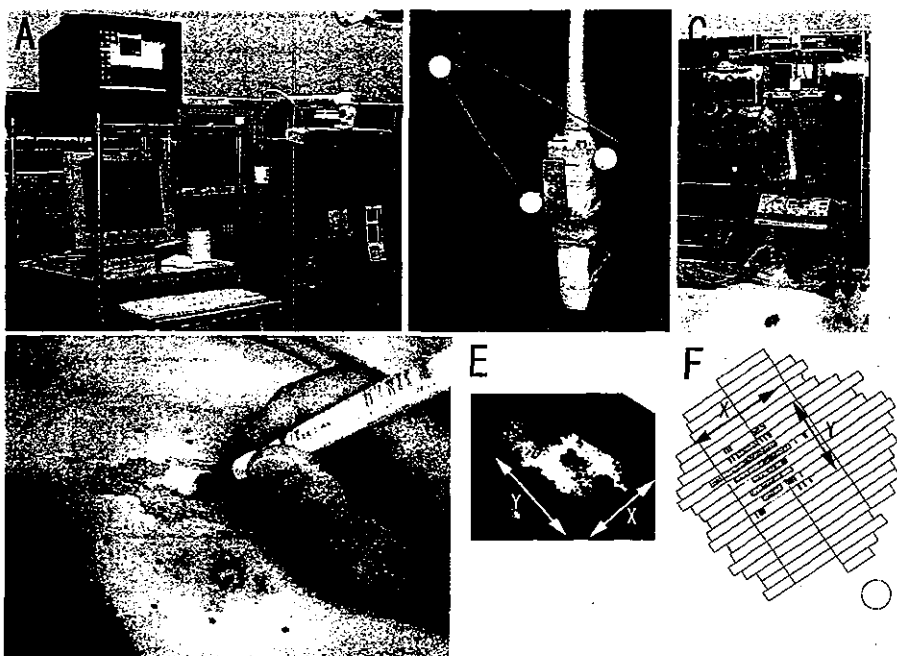


Fig 4. The real-time ultrasound navigation system is constructed of Polaris, a workstation (A), a ultrasound probe with reflection balls for Polaris (B) and a video camera (C). The reconstructed tumor image is superimposed on the patient's video image (D). The tumor size was measured in two directions using the 3D image (E) and pathological mapping (F).

system consisted of a Polaris (Northern Digital, Waterloo, Canada) 3D locator, a video camera and a workstation. The 10 MHz linear probe and the video camera were attached to a small acrylic panel with reflection balls for the Polaris (Fig 4A, 4B, 4C). All procedures were performed in an operating room just before surgery as reported previously^{5,6}. Briefly, under general anesthesia, the patient was placed in the supine position for breast cancer surgery with her arm fixed above her face.

Ultrasound images were acquired and data regarding geometrical location recorded. The region of interest (ROI) containing the tumor was cut out from each 2D image. A 3D image was obtained from the batch of these 2D images of ROI by volume rendering. A three-dimensional tumor image was extracted using the opacity reference obtained from the 2D tumor image, and was then superimposed onto the video image of the patient (Fig 4D). Tumor size was measured in 2 directions,

one parallel to the line connecting the nipple and the tumor and one orthogonal to this line (Fig 4E, 4F). Assessment and measurement of 3D images was performed using Virtual Place software (Medical Imaging Laboratory, Tokyo, Japan), and the statistical analysis was performed using Statview software (SAS Institute, Cary, NC).

Pathological examination was done by a pathologist at each institute. Specimens were prepared according to the General Rules for Clinical and Pathological Recording of Breast Cancer published by the Japanese Breast Cancer Society. The resected tissue was sliced into 5-mm thick specimens, and pathological mapping of the tumor was performed. Tumors with intraductal components spreading over 2 cm from the edge of the invasive lesion were determined as ISC positive. Three-dimensional images were compared with these maps of the tumor, and assessed.

Results

Three-D helical CT examination was performed for 52 primary breast cancer patients. Among them, 47 had invasive ductal carcinoma and 5 had ductal carcinoma *in situ* (DCIS). Seventeen tumors were pathologically proven to be DCIS or to have ISC, and 11 of them were detected by 3D helical CT (sensitivity = 64.7%). Only one patient was suspected to have ISC by 3D helical CT of 35 ISC-negative patients (specificity = 97.1%). The diagnostic accuracy was 86.5% (Table 1).

The diagnostic ability of 3D MRI for ISC was assessed in 76 primary breast cancer patients with invasive ductal carcinoma. Thirty-seven patients were diagnosed as having tumors with ISC by 3D MRI out of 41 having tumors with pathologically proven ISC (sensitivity = 90.2%). Thirteen out of 35 tumors without ISC were suspected to have ISC by MRI (specificity = 62.9%). The diagnostic accuracy of 3D MRI for ISC was 77.6% (Table 2).

Three-D ultrasound examination was performed for 42 primary breast cancer patients. Among 14 pathologically ISC positive tumors, 11 were detected by MPR images (sensitivity = 78.6%). The specificity and diagnostic accuracy were 100% and 92.3% respectively (Table 3).

A historical comparison of the effect of 3D helical CT navigation on breast conserving surgery is summarized in Table 4. Helical CT navigation reduced the positive rate of surgical margins from 40% to 18%.

Table 1. Diagnostic Ability of 3D Helical CT for ISC*

	Pathology	
	Positive	Negative
CT Positive	11	1
CT Negative	6	34

*ISC; intraductal spread of cancer

Table 2. Diagnostic Ability of 3D MRI for ISC*

	Pathology	
	Positive	Negative
MRI Positive	37	13
MRI Negative	4	22

*ISC; intraductal spread of cancer

Table 3. Diagnostic Ability of 3D US for ISC*

	Pathology	
	Positive	Negative
US Positive	11	0
US Negative	3	28

*ISC; intraductal spread of cancer, US; ultrasound

Table 4. Comparison of Positive Ratio of Surgical Margin Before and After Application of 3D CT Navigation

	Application of 3D CT navigation	
	Before	After
Margin Positive/Total (%)	15/38 (39.5)	20/109 (18.3)

Table 5. Result of 3D MRI Navigation Surgery for Non-Palpable Breast Cancer

Margin Positive/Total (%)	4/12 (33.3)
---------------------------	-------------

Three-D MRI navigation was performed for patients with non-palpable breast cancer showing microcalcification detected by mammography. Twelve patients were examined, and all tumors were clearly displayed by MRI. Out of 12 tumors, 8 could be removed with negative surgical mar-

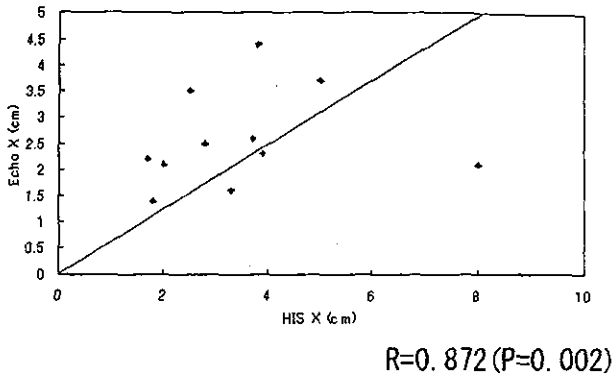


Fig 5. Tumor size by 3D ultrasound correlates with the pathological tumor size ($R=0.872$).

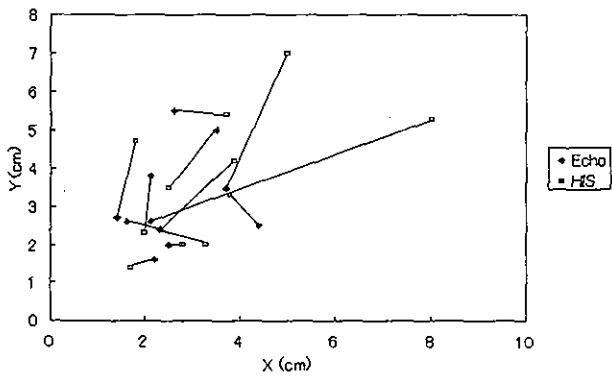


Fig 6. Scattered plot of tumor size in two directions by both 3D images and pathological mapping. The distance between two dots was measured, and was less than 2 cm in 8 out of 11 tumors.

gins using MRI navigation (Table 5).

Real-time 3D ultrasound navigation was performed for 32 patients with primary breast cancer. The time needed for navigation was about 20 minutes⁹. Among 32 tumors, 9 tumors had pathologically proven ISC and 4 were DCIS. Eleven out of these 13 tumors could be clearly visualized and their sizes measured. One of 2 tumors which were not displayed clearly was a widely spreading DCIS, and the other was a small invasive ductal cancer with extensive intraductal component widely spreading in the upper quadrants. The size of the tumors on 3D images measured in a single direction correlated with pathological tumor size ($R=0.872$, $p=0.002$) (Fig 5). The tumor size in two directions by 3D ultrasound and the pathological specimen sizes are shown in Fig 6. In 8 out of 11 cases, the differences between the two were less than 2 cm (72.7%).

Discussion

Computer technology has allowed 3D images to be easily obtained and analyzed by means of not only a specialized workstation but also a personal computer. Computed tomography and MRI acquire and reconstruct digital data, and are suitable modalities for 3D diagnosis. Recently, these 3D imaging modalities including helical CT, MRI and 3D ultrasound have been applied for breast cancer diagnosis. For breast cancer, 3D images are useful for delineating cancer location and spread rather than for differentiating cancer from benign lesions. However, it is fact that each modality has both strong and weak points for detecting ISC. From previous reports regarding ISC, MRI is considered to be superior to CT in terms of sensitivity, but inferior in specificity^{7,12}. The sensitivity is higher than the specificity with MRI, while the sensitivity is lower than the specificity with CT. In our series, the same tendency was observed. The sensitivity of 3D helical CT for ISC was 64.7%, lower than its specificity (97.1%), and the specificity of 3D MRI (62.7%) was lower than the sensitivity (90.2%). Three-D helical CT seemed superior to MRI for detecting ISC in terms of diagnostic accuracy (86.5% vs. 77.6%). However, the patients enrolled were different in each modality group in our series, so we can not conclude which is more suitable for ISC detection.

On the other hand, 3D ultrasound has become commercially available very recently. We examined the patients with MPR images, and showed high sensitivity and specificity. Ultrasound has several advantages in that it is real-time, non-invasive, repeatable, and easy to use during surgery. However, the current commercially-provided system does not have a system for sensing 3D location. Therefore, the obtained 3D volume data were mechanically reconstructed to a cuboidal form, which cannot reflect the real shape of cancer. Furthermore, the width of the probe is so narrow that it cannot scan both widely-spreading and multiple tumors completely. At present, it seems suitable for small tumors with intraductal spread in one direction.

Even if a clear 3D image of breast cancer is obtained, it is of no use during surgery without superimposing it on the patient's body. Three-D navigation is one of the most expecting future technologies. We tried to assess the feasibility of

each modality, but the system and data are preliminary.

Navigation by 3D helical CT was performed by correcting the marking indicating tumor spread prepared by a surgeon's palpation. This could potentially reduce the number of positive surgical margins in breast conserving surgery, though the data were obtained by historical comparison. This method seems easy to perform with no additional special equipment. It should be acceptable in most general hospitals.

For non-palpable lesions, complete but minimal resection of the tumor with free margins is difficult. We tried a new navigation technique using MRI and a special mapping sheet⁴⁾. In this system, patients were placed in the spine position, and the skin marking for tumor removal was performed by inking the grids containing the tumor image. By means of this method, 8 out of 12 lesions (66.7%) were removed without positive margins. Of course this was very preliminary, and we should accumulate more data to assess this system.

One problem with navigation techniques mentioned above is that there must be some difference in the patient's position between navigation and surgery, which may result in misleading. To overcome this problem, we developed a real-time navigation system using 3D ultrasound in the operating room^{5,6)}. In this system, the data were obtained from a patient positioned for the surgery under general anesthesia. There is no discrepancy caused by differences in the patient's position. Because ultrasound images provide no geometrical data in 3D space, we applied a positioning system and acquired the image along with geometrical data in the workstation. A three-D image of the tumor was reconstructed by volume rendering based on this geometrical data, and finally superimposed onto a video image of the patient. These 3D images should reflect the real shape of tumor in the breast, which is completely different from those obtained by currently available ultrasound machines. The difference in tumor size between the 3D image and the pathological specimen was less than 2 cm in 8 out of 11 tumors (72.7%). This indicates that 3D ultrasound navigation could be reliable in clinical application. However, this data was slightly less promising than that obtained for contrast enhanced CT examination¹³⁾. Ultrasound images contain noise caused by anatomical structures of the breast and therefore technical fail-

ures. Furthermore, there are no suitable contrast enhanced media for ultrasound examination of the breast. This might cause the slight inferiority of visualization by 3D ultrasound compared with CT. However, the superimposing system seemed to have a great advantage in that it could show likely image of the tumor to a surgeon, and therefore be very useful for decision making for tumor resection. We are now trying to use 3D CT images obtained preoperatively in this navigation system as well as ultrasound images, and this hybrid system would provide more accurate information for navigation.

Three-D imaging and diagnosis of ICS can be reliable, if it is performed based on 2D images or images obtained by other modalities. It seems useful for surgical decision-making in breast conserving surgery, because it can show likely and direct image of tumor spread. However, to apply these images for real-time intraoperative navigation, many technical problems including methods for displaying the image must be solved. Furthermore, a prospective study with more patients should be done to confirm its reliability.

Acknowledgement

This study was supported by the Japanese Breast Cancer Society.

References

- 1) Spivack B, Khanna MM, Tafta L, Juillard G, and Giuliano AE: Margin status and local recurrence after breast-conserving surgery. *Arch Surg* 129:952-956, 1994.
- 2) Luu HH, Otis CN, Reed WP, Garp JL, and Frank JL: The unsatisfactory margin in breast cancer surgery. *Am J Surg* 178:362-366, 1999.
- 3) Uematsu T, Sano M, Homma K, Shiina M, and Kobayashi S: Three-dimensional helical CT of the breast: accuracy for measuring extent of breast cancer candidates for breast conserving surgery. *Breast Cancer Res Treat* 65:249-257, 2001.
- 4) Nakamura S, Kenjo H, Nihio T, Kazama T, Doi O, and Suzuki K: 3D-MR mammography-guided breast conserving surgery after neoadjuvant chemotherapy: clinical results and future perspectives with reference to FDG-PET. *Breast Cancer* 8:351-354, 2001.
- 5) Tamaki Y, Sato Y, Nakamoto M, Sasama T, Sakita I, Sekimoto M, Ohue M, Tomita N, Tamura S, and Monden M: Intraoperative navigation for breast cancer surgery using 3D ultrasound images. *Comput Aided Surg* 4:37-44, 1999.
- 6) Sato Y, Nakamoto M, Tamaki Y, Sasama T, Sakita I, Nakajima Y, Monden M, and Tamura S: Image guidance of breast cancer surgery using 3-D ultrasound images and augmented reality visualization. *IEEE Tran Med Imaging* 17:681-693, 1998.

- 7) Satake H, Shimamoto K, Sawaki A, Niimi R, Ando Y, Ishiguchi T, Ishigaki T, Yamakawa K, Nagasaka T, and Funahashi H: Role of ultrasonography in the detection of intraductal spread of breast cancer: correlation with pathologic findings, mammography and MR imaging. *Eur Radiol* 10:1726-1732, 2000.
- 8) Akashi-Tanaka S, Fukutomi T, Miyakawa K, Uchiyama N, Nanasawa T, and Tsuda H: Clinical use of contrast-enhanced computed tomography for decision making in breast conserving surgery. *Breast Cancer* 4:280-284, 1997.
- 9) Akashi-Takaka S, Fukutomi T, Miyakawa K, Uchiyama N, and Tsuda H: Diagnostic value of contrast-enhanced computed tomography for diagnosing the intraductal component of breast cancer. *Breast Cancer Res Treat* 49:79-86, 1998.
- 10) Tozaki M, Yamashita A, Kawakami M, Yoshida K, Yamazaki Y, and Fukuda K: Diagnosis of breast cancer extent using dynamic multidetector-row CT: correlation between MPR imaging and pathological cross-sections. *Nippon Igaku Hoshasen Gakkai Zasshi* 60:560-567, 2000 (in Japanese with English abstract).
- 11) Hiramatsu H, Enomoto K, Ikeda Y, Mukai M, Furuta T, Hattori H, Tanami Y, Ohashi T, Kitajima M, and Hiramatsu K: Three-dimensional helical CT for treatment planning of breast cancer. *Radiat Med* 17:35-40, 1999.
- 12) Uematsu T, Sano M, Homma K, Mokino H, Shiina M, Kobayashi S, and Shimizu K: Staging of palpable T1-2 invasive breast cancer with helical CT. *Breast Cancer* 8:125-130, 2001.
- 13) Akashi-Tanaka S, Fukutomi T, Miyakawa K, Nanasawa T, Matsuo K, Hasegawa T, and Tsuda H: Contrast-enhanced computed tomography for diagnosing the intraductal component and small invasive foci of breast cancer. *Breast Cancer* 8:10-15, 2001.

1.

乳癌の診断

(1) 乳癌の画像診断；最近の進歩

聖路加国際病院外科

中村 清吾

Seigo Nakamura

はじめに

乳癌の画像診断としては、従来よりマンモグラフィと超音波が広く一般に普及し、早期癌の発見にも寄与してきた。

さらに最近では、MRI (MR mammography) やヘリカルCTも乳癌の診断に用いられるようになり、とくに、乳房温存療法を念頭においた癌の広がり診断への応用が期待されている。そこで、本項では、各種画像診断の可能性と限界についてレビューする。

早期乳癌発見の意義

乳癌の予後因子としては、最近各種遺伝子マーカーをはじめとして、様々なものが研究されているが、いまだリンパ節転移に優るものがないのが現状である。そのリンパ節転移に関しては、やはり大きさに比例することが知られている。腫瘍径1cm未満の場合にリンパ節転移を伴っているのは、20%以下である。さらに、病理学的に非浸潤癌というレベルで発見し、手術を中心とする処置を行えば、理論的に転移する可能性はほとんどなく、根治が期待できる。そこで、非浸潤癌や、せめて1cm以下の浸潤癌のレベルで乳癌を発見で

きるか否かが、画像診断上きわめて重要である。

微細石灰化病変のマンモグラフィ診断

非浸潤癌の大多数は、マンモグラフィによる微細石灰化病変もしくは、血性乳頭分泌の精査により発見される。そこで、画像診断上は、石灰化病変の検出率がどの程度かということが問題となる。悪性石灰化像の指標としては、従来より、Eganの3基準として、①微細、②集簇、③多数が知られてきたが、大きさは、100~300 μ で、大小不同であり、形状は多様で、砂粒状のほか、線状や、乳管の分岐を鋳型にしたY字型のものまである。また、集簇とは5mm²に10個以上認められる場合を称する。

通常のスクリーンフィルム系のマンモグラフィでは、理論的に25~50 μ 程度までの解像度が得ら

れ、石灰化の数や形状を把握して、ある程度の良悪性の鑑別を行うことができる。

近年登場したデジタルマンモグラフィは、X線で得られた画像情報をCCDを含む特殊センサーで受け取り、信号をデジタル化して、ディスプレイに映し出したり、コンピュータによる画像解析を可能とする。画像情報は、ピクセル(pixel)という単位で処理されるが、例えば18×24cmのマンモグラフィ一枚を50 μ の解像度で表現するためには、3,600×4,800ピクセルが必要である。さらに、各ピクセルが、10~12bit(1024~4096階調)の濃度情報を有するとすれば、コンピュータの記憶容量としては、3,600×4,800×2¹⁰≈約16Gbyteもの大容量が必要となる(注：圧縮技術などを用いない単純計算)。この点が、CTやMRIのデジタル化と決定的に異なる点であり、石灰化の描出と

図1 3D-MRIの撮影条件

MRI本体：GE SIGNA1.5T
使用コイル：breast phased array coil
シーケンス：EFGRE3D (enhanced fast gradient echo 3D)
TR6.7ms, TE1.7ms, TI40ms, FA15° 256×160matrix
スライス厚：1mm, FOV：16cm

Gdは、オートインフューザによる注入
オプション：SPECIAL (special inversion at lipids)
撮像時間：約90秒

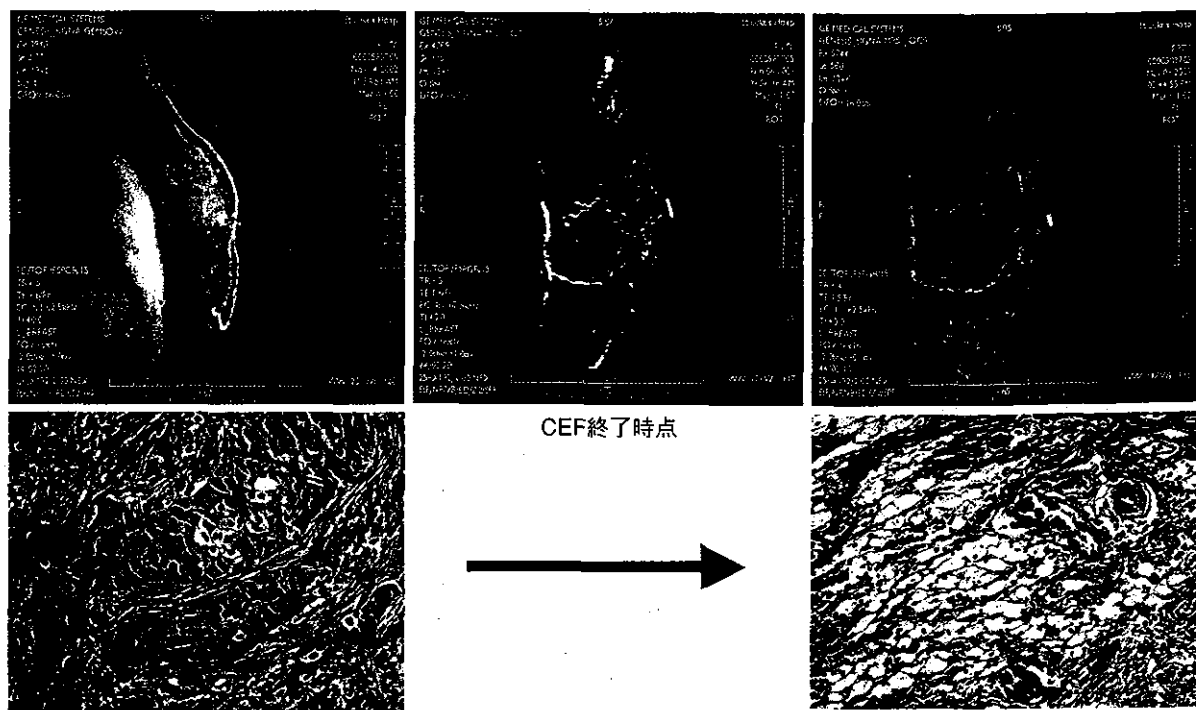


図1 CEF→DOCにて、pCRが得られた1例

いうことを目標としているマンモグラフィがPACS (picture archiving and communication system) 上で扱いきれないといわれるゆえんである。しかし、ステレオガイド下生検を行うため開発された専用ディスプレイ ($2 \times 2K = 2,048 \times 2,048$ pixels) では、約1/4程度の解像度になるものの、関心領域を絞り込んで、その部位のみ拡大して観察するなどの工夫をして解像度の低さを補っている¹⁾。

一度デジタル化すれば、コンピュータによる画像解析が可能となり、診断支援システムが期待できる。カリフォルニア州に本社のあるR2Technologyという会社は、The Image-Checker Systemというマンモグラフィの読影を支援するシステムを開発した。本システムでは、5人の放射線診断医が乳癌と診断した病変の83%を正しくとらえ、逆に専門医が見逃した15%の乳癌病変のうち、85%を正しくとらえることが可能であった。したがって、放射線診断医を支援する

システムとして、近い将来普及する可能性がある^{2)~4)}。

超音波による微小石灰化病変の診断

石灰化の描出を中心にとらえるとき、マンモグラフィが画像診断の中心となるが、乳癌は必ずしも石灰化を伴うとは限らず、とくに乳房温存療法を前提とした場合、乳管内進展病変の診断が重要である。超音波では、主腫瘍から連続して伸びる壁不整な管状構造物や、娘結節を様々な角度から、動的に観察できるというメリットがある。さらに最近では、カラードップラーを利用することで、血流シグナルをとらえ、血管量、血流速度などから微小病変の同定に役立つようという研究が進んでいる。また、血球から跳ね返ってくる散乱波エネルギーをシグナル化したパワードップラー法により、より細い血管や低流速の血流が可視化できるようになった。これに加えて、米国では、レボビストな

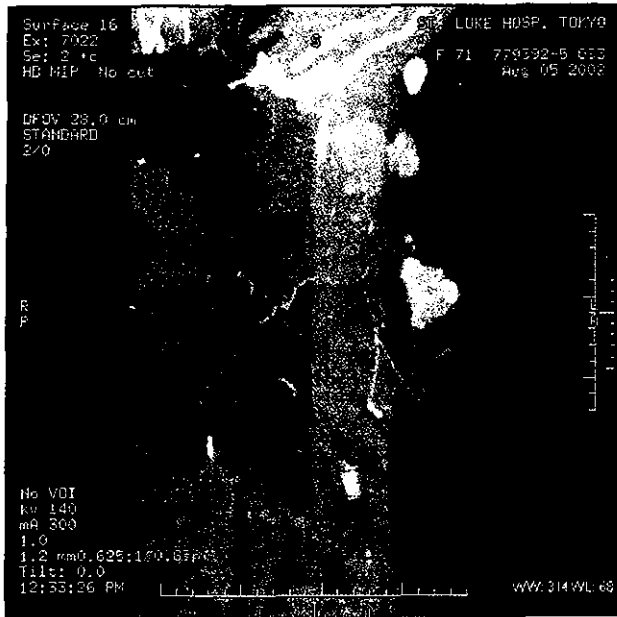
どの経静脈性の造影剤を用いることで、カラーシグナルを増強することなどが試みられている。

超音波の現状における解像度は、 300μ 前後が限界であり、石灰化の存在診断はある程度可能であるが、濃度や形状を細部に評価することは困難である。むしろ、石灰化病変に一致して、微小腫瘍や拡張した乳管構造を認めるか否かといった超音波検査の特徴を考慮した利用法が望ましい。

MRIおよびCT

MRIの分解能は、機械や撮像方法により様々であるが、当院におけるMRIの撮像方法と、空間分解能を表1に示す。解像度としては、マンモグラフィに比しかなり劣る。

しかし、MRIは組織分解能に優れており、Gd造影MRIにより、90秒~3分以内に撮影するイメージでは、正常乳腺との識別が容易となり、とくにマンモグラフィでdense

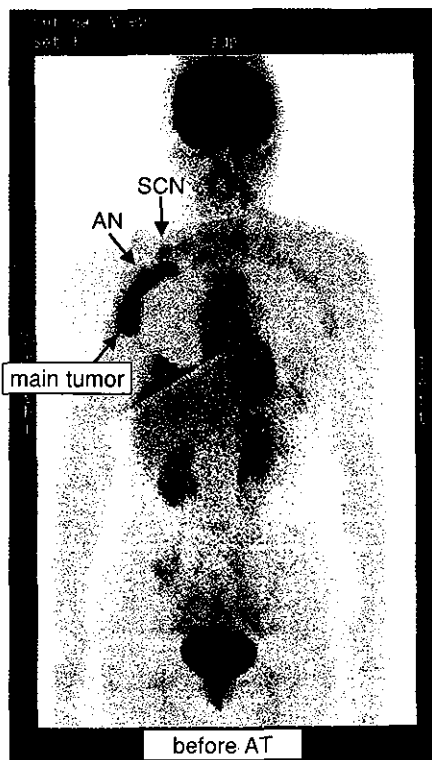


アナストロゾール投与前



アナストロゾール投与6カ月後

図 2



before AT



after AT

図 3

breastと称される場合でも、その内部に含まれる腫瘍をより明瞭に描出することが可能である。またMRIは、そもそも石灰化自体を描出することはできない。しかし、石灰化は本来、乳管内病変の一部を構成しているものである。した

がって、周囲の新生血管量や透過性の亢進、その血流を反映していると考えられる。そこで、Gd造影MRIはマンモグラフィで指摘された微小石灰化を含む乳管内病変の全貌をとらえ、広がり診断に役立つ⁹⁾。しかし、ここで気をつけな

なければならないことは、良性病変でも増生能が活発な病変ではGdにて造影されることがあり、特異度 (specificity) が若干劣る点である。そこで、温存手術時の広がり診断に用いた際、主病巣からかなり離れた部位に娘結節が疑われた場合